

**OMTM, Volume 23**

**Supplemental information**

**Modulating immune responses to AAV by expanded  
polyclonal T-regs and capsid specific  
chimeric antigen receptor T-regulatory cells**

**Motahareh Arjomandnejad, Katelyn Sylvia, Meghan Blackwood, Thomas Nixon, Qiushi Tang, Manish Muhuri, Alisha M. Gruntman, Guangping Gao, Terence R. Flotte, and Allison M. Keeler**

## Supplemental Information

### This PDF file includes:

Supplemental Material and Methods

Figures S1 to 12

Tables S1 and S2

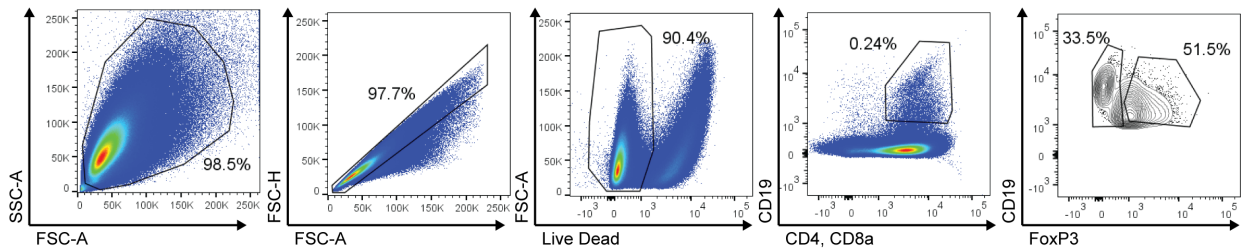
### Supplemental Material and Methods

#### Genomic DNA extraction and quantitative-PCR

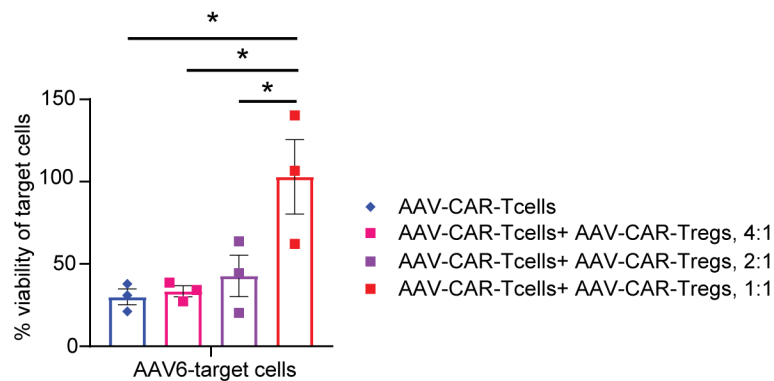
DNA was extracted from the injected muscle using Qiagen Puregene Core Kit A (158667) and quantified as previously described <sup>1</sup>.

#### Immunohistochemistry

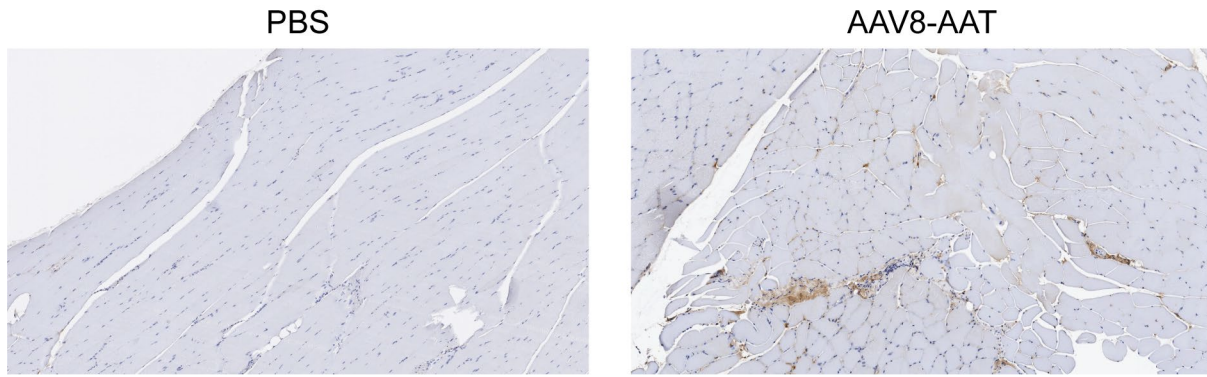
Immunohistochemical staining to detect caspase-3 within myofibers as well as D3 staining were performed after tissues were fixed in 10% neutral buffered formalin for 24 hours at the room temperature (Fisher Scientific, Waltham, MA, USA) and embedded in paraffin by University of Massachusetts Medical School Morphology Core (Worcester, MA, USA) or Molecular Pathology Core at University of Florida. AAV antibody (D3 monoclonal antibody) was used to identify the AAV virus in mouse tissues without permeabilization and tissues were treated with mouse IgG to eliminate endogenous mouse IgG. Sections were incubated with mouse anti-AAV (D3) antibody followed by incubation with biotinylated goat anti-mouse immunoglobulin antibodies (Vector, Burlingame, CA). For caspase-3 staining cleaved caspase-3 antibody (Cell Signaling, Danvers, MA) was used, and permeabilization was performed prior to antibody staining.



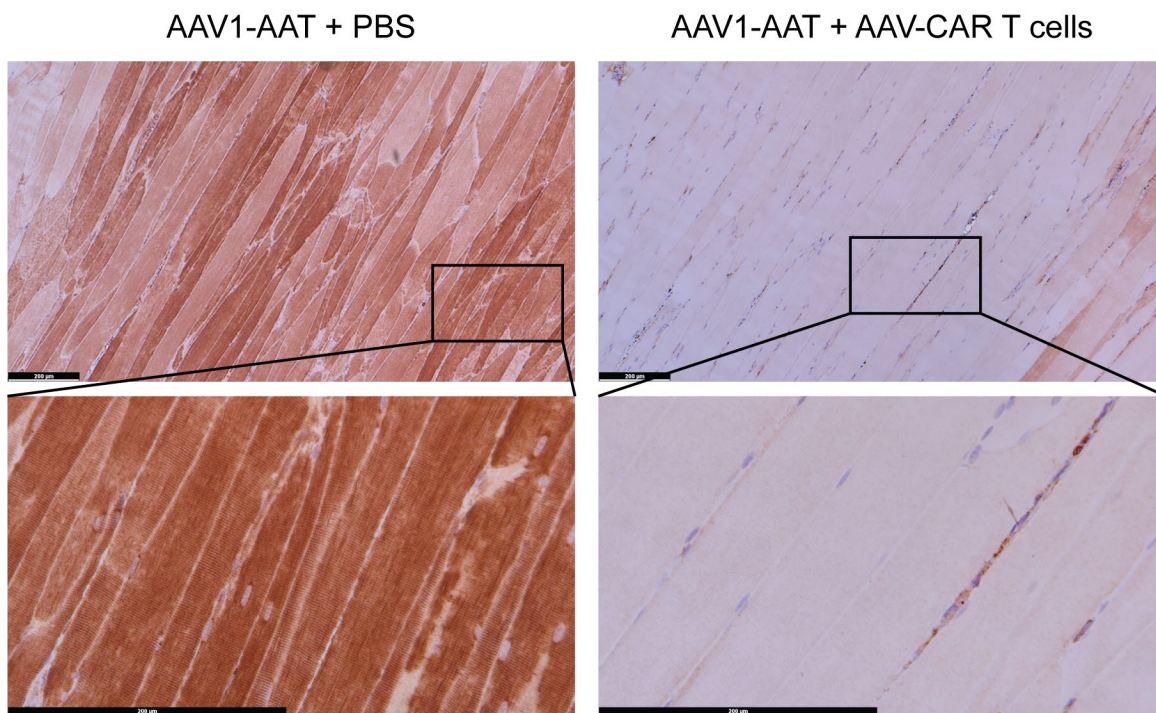
**Figure S1. Gating strategy for AAV-CAR Tregs.** Panels show representative FACS profiles of 3 independent experiments using human samples from 3 healthy donors.



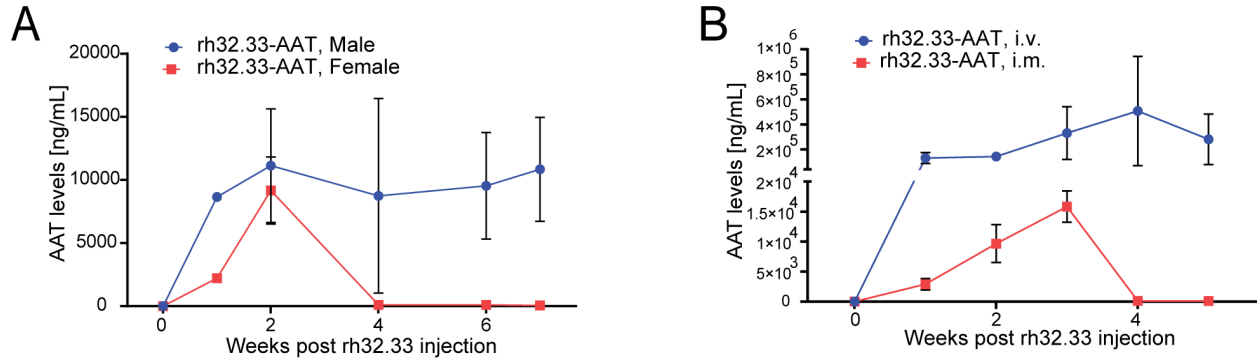
**Figure S2. Suppressive activity of AAV-CAR Treg is dose dependent.** Cytotoxicity of AAV-CAR T cells (blue bars) and suppression of cytotoxicity by AAV-CAR Tregs against AAV6-target cells as read by cell viability. Percent viability is determined by luciferase expression measured 24 hours after coculture. Cells were cultured at a ratio of 1:10 target cell to AAV-CAR T cell and 4:1, 2:1 and 1:1 of AAV-CAR T cell to AAV-CAR Treg. Data are the average of 3 independent experiments using human samples from 3 healthy donors (within each experiment samples were run in triplicate). Error bars are mean  $\pm$  SEM; \*  $p \leq 0.05$  by two-way ANOVA with Tukey's multiple comparisons.



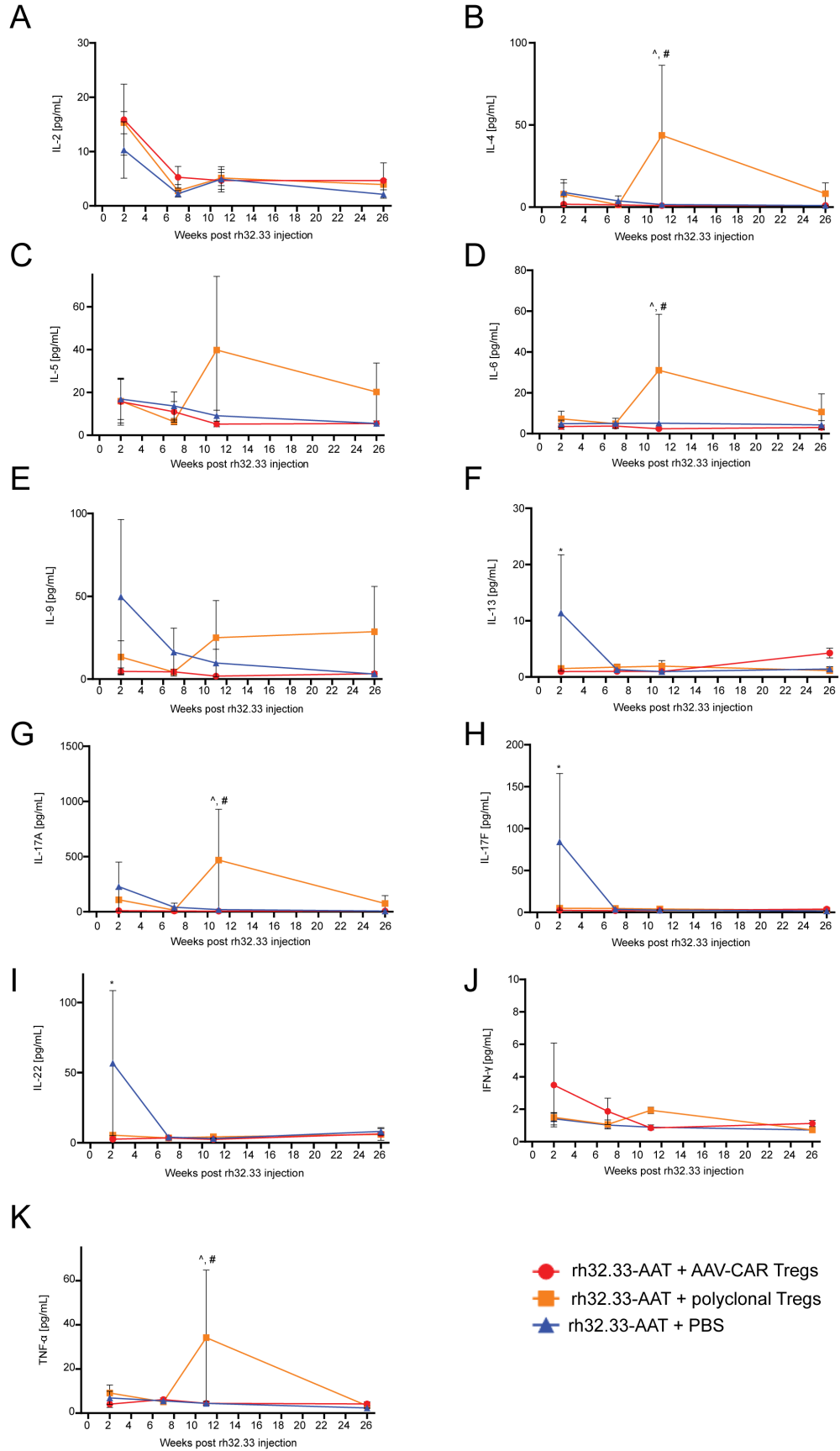
**Figure S3. D3 staining of injected muscles.** Representative images of D3-stained limb muscles without permabilization of mice 3 months post i.m. injection with AAV8-AAT.



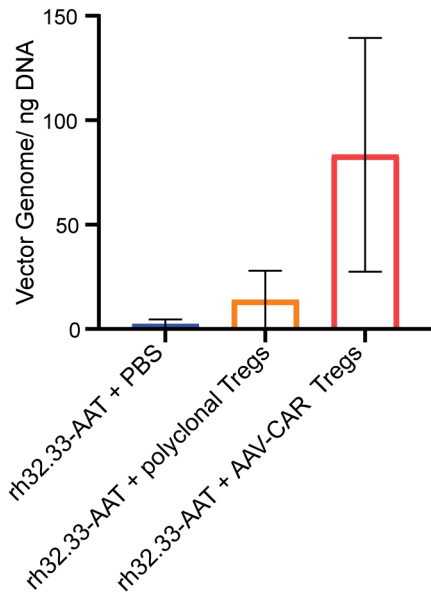
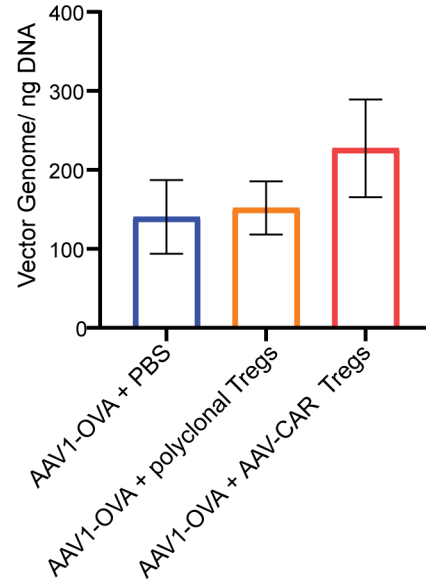
**Figure S4. AAV-CAR T cells clears AAT expression in vivo.** Representative images of AAV1-AAT injected muscles stained by immunohistochemistry for AAT protein (brown), 6 weeks after AAV injection. Scale bars are 200  $\mu$ m.



**Figure S5. Clearance of AAT expression in i.m. injected female C57BL/6. A.** Serum levels of AAT in male and female animals receiving rh32.33-AAT measured by ELISA. **B.** Serum levels of AAT in i.m. and i.v. injected animals measured by ELISA (n=3).



**Figure S6. CBA assay analysis of animal serum (capsid specific immune response experiment).** **A.** Serum levels of IL-2 measured by CBA assay over time. **B.** Serum levels of IL-4 measured by CBA assay over time. **C.** Serum levels of IL-5 measured by CBA assay over time. **D.** Serum levels of IL-6 measured by CBA assay over time. **E.** Serum levels of IL-9 measured by CBA assay over time. **F.** Serum levels of IL-13 measured by CBA assay over time. **G.** Serum levels of IL-17A measured by CBA assay over time. **H.** Serum levels of IL-17F measured by CBA assay over time. **I.** Serum levels of IL-22 measured by CBA assay over time. **J.** Serum levels of IIFN- $\gamma$  measured by CBA assay over time. **K.** Serum levels of TNF- $\alpha$  measured by CBA assay over time. Two-way ANOVA with Tukey's multiple comparisons was used (n=6 for AAV-CAR Treg and PBS treated groups, n=5 for polyclonal Treg treated group for A, B, C, D, E, F, G, H, I, J and K). Error bars are mean  $\pm$  SEM; \*  $p \leq 0.05$ . \*: AAV-CAR Tregs compared to PBS, #: AAV-CAR Tregs compared to polyclonal Tregs and ^: polyclonal Tregs compared to PBS.

**A****B**

**Figure S7. Vector genome quantification of injected muscles. A.** Quantitative-PCR for vector genome shows greater transduction in the rh32.33-AAT injected muscles of the animals treated with AAV-CAR Tregs, with less vector genomes evident in polyclonal Treg and PBS treated groups. Error bars  $\pm$  SEM (n=2) (samples were run in triplicate). **B.** Quantitative-PCR for vector genome shows greater transduction in the AAV1-OVA injected muscles of the animals treated with AAV-CAR Tregs, with less vector genomes evident in polyclonal Treg and PBS treated groups. Error bars  $\pm$  SEM (n=5 for AAV-CAR Treg and polyclonal treated groups and n=2 for PBS treated group) (samples were run in triplicate).



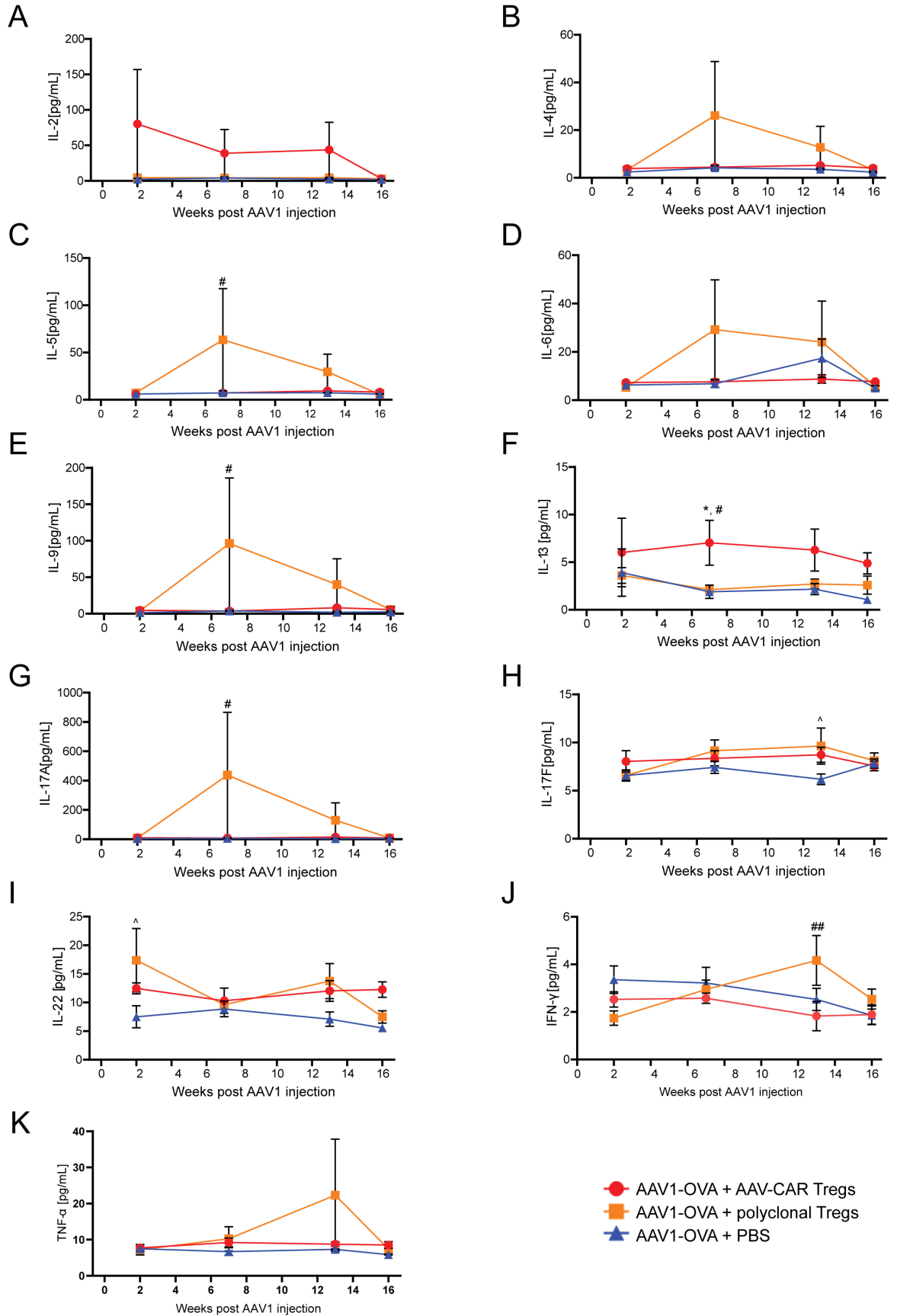


**Figure S8. CBA assay analysis of animal serum (delivered- transgene immune response experiment).** **A.** Serum levels of IL-2 measured by CBA assay over time. **B.** Serum levels of IL-4 measured by CBA assay over time. **C.** Serum levels of IL-5 measured by CBA assay over time. **D.** Serum levels of IL-6 measured by CBA assay over time. **E.** Serum levels of IL-9 measured by CBA assay over time. **F.** Serum levels of IL-13 measured by CBA assay over time. **G.** Serum levels of IL-17A measured by CBA assay over time. **H.** Serum levels of IL-17F measured by CBA assay over time. **I.** Serum levels of IL-22 measured by CBA assay over time. **J.** Serum levels of IFN- $\gamma$  measured by CBA assay over time. **K.** Serum levels of TNF- $\alpha$  measured by CBA assay over time. Two-way repeated-measure ANOVA with Tukey's multiple comparisons was used (n=5 for AAV-CAR Treg and polyclonal Treg treated groups, n=3 for the PBS treated group for A, B, C, D, E, F, G, H, I, J and K). Error bars are mean  $\pm$  SEM; \*  $p \leq 0.05$ . \*: AAV-CAR Tregs compared to PBS, #: AAV-CAR Tregs compared to polyclonal Tregs and ^: polyclonal Tregs compared to PBS.

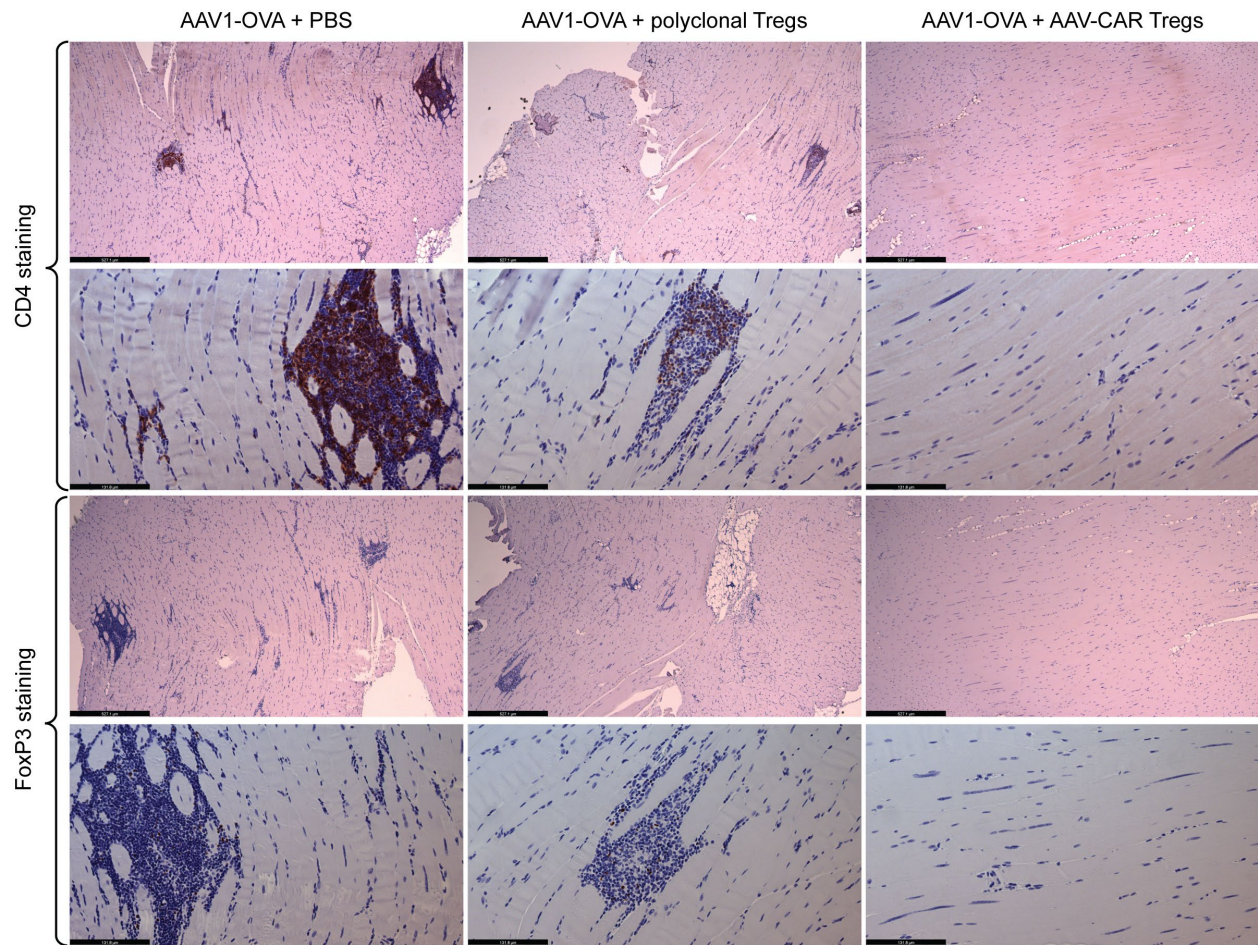


**Figure S9. CD4 and FoxP3 staining of injected muscles (delivered- transgene immune response experiment).** Representative images of CD4 and FoxP3-stained limb muscles of mice 16 weeks post i.m. injection with AAV1-OVA. Upper panels for CD4 and FoxP3 staining 527  $\mu\text{m}$  scale bar, lower panels for CD4 and FoxP3 staining 131  $\mu\text{m}$  scale bar.

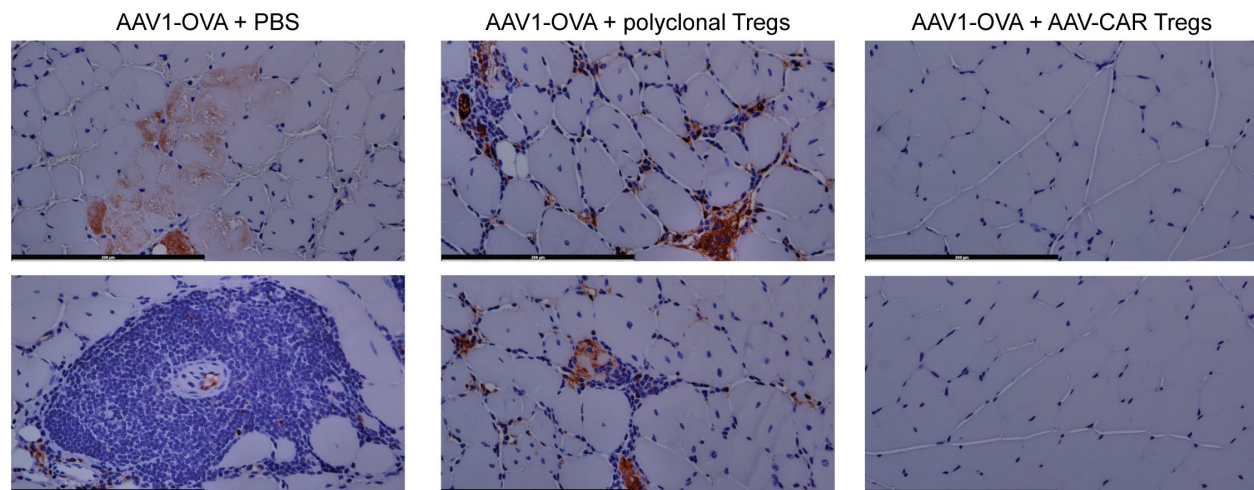


**Figure S10. Representative caspase-3 staining in muscles.** Representative images of Caspase-3-stained limb muscles of mice 16 weeks post i.m. injection with AAV1-OVA. 200  $\mu$ m scale bar.

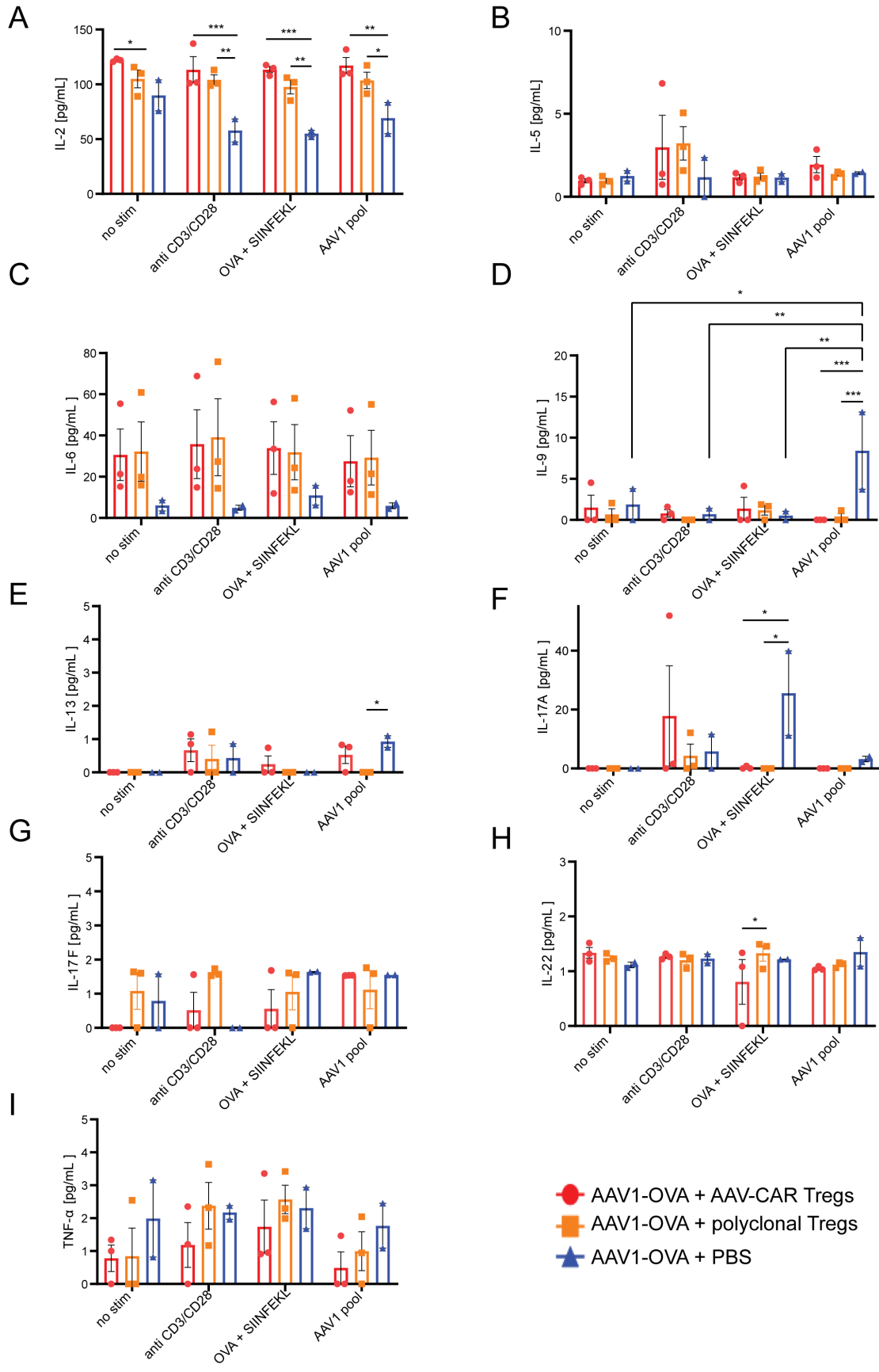


**Figure S11. CBA assay analysis of culture supernatant (muscle).** **A.** IL-2 levels in the supernatant measured by CBA assay. **B.** IL-5 levels in the supernatant measured by CBA assay. **C.** IL-6 levels in the supernatant measured by CBA assay. **D.** IL-9 levels in the supernatant measured by CBA assay. **E.** IL-13 levels in the supernatant measured by CBA assay. **F.** IL-17A levels in the supernatant measured by CBA assay. **G.** IL-17F levels in the supernatant measured by CBA assay. **H.** IL-22 levels in the supernatant measured by CBA assay. **I.** TNF- $\alpha$  levels in the supernatant measured by CBA assay. Two-way ANOVA with Tukey's multiple comparisons was used (n=3 for AAV-CAR Treg and polyclonal Treg treated groups, n=2 for the PBS treated group for A, B, C, D, E, F, G, H and I). Error bars are mean  $\pm$  SEM; \*  $p \leq 0.05$ , \*\*  $p \leq 0.01$ , \*\*\*  $p \leq 0.001$ .

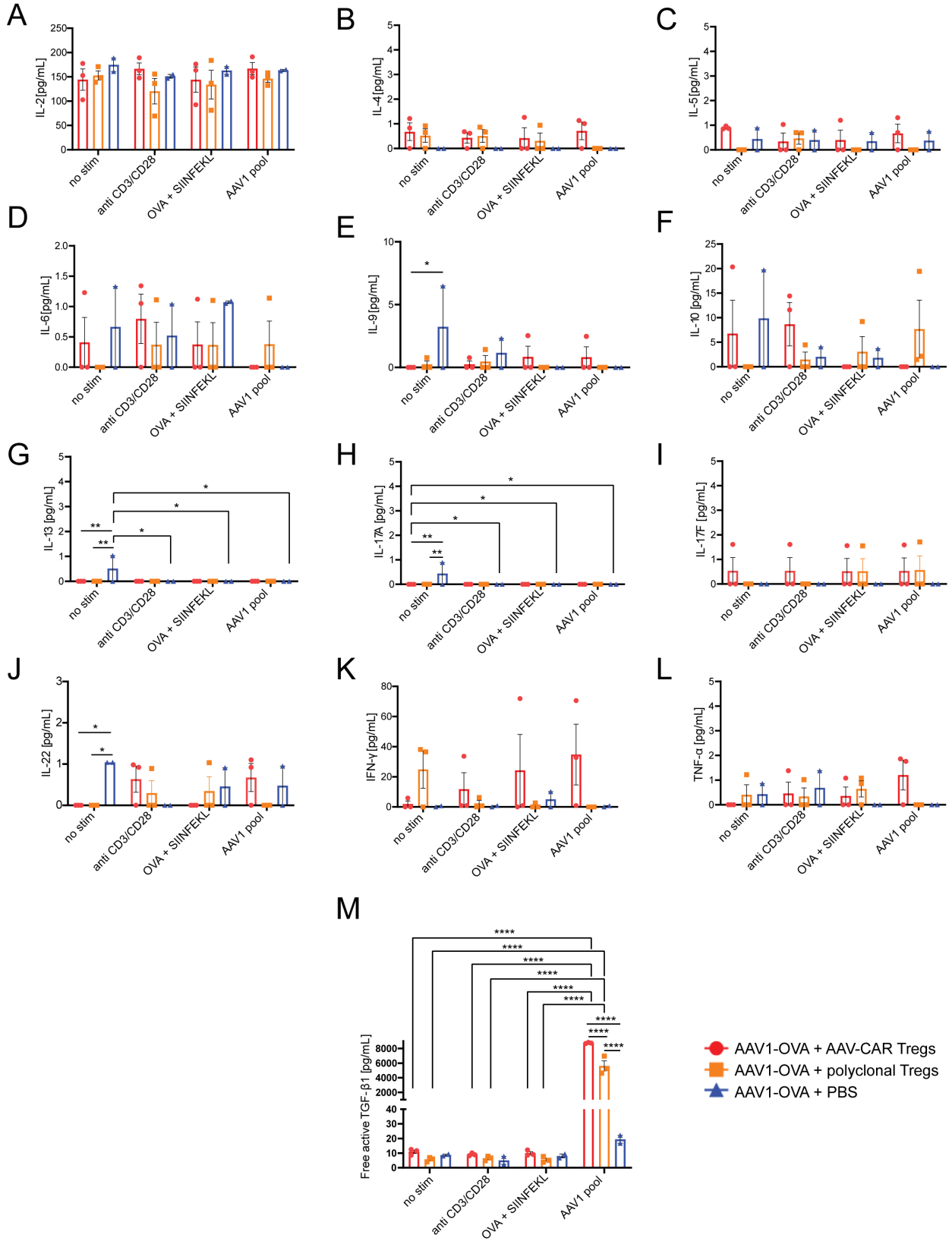


**Figure S12. CBA assay analysis of culture supernatant (spleen).** **A.** IL-2 levels in the supernatant measured by CBA assay. **B.** IL-4 levels in the supernatant measured by CBA assay. **C.** IL-5 levels in the supernatant measured by CBA assay. **D.** IL-6 levels in the supernatant measured by CBA assay. **E.** IL-9 levels in the supernatant measured by CBA assay. **F.** IL-10 levels in the supernatant measured by CBA assay. **G.** IL-13 levels in the supernatant measured by CBA assay. **H.** IL-17A levels in the supernatant measured by CBA assay. **I.** IL-17F levels in the supernatant measured by CBA assay. **J.** IL-22 levels in the supernatant measured by CBA assay. **K.** IFN- $\gamma$  levels in the supernatant measured by CBA assay. **L.** TNF- $\alpha$  levels in the supernatant measured by CBA assay. **M.** Free active TGF- $\beta$ 1 levels in the supernatant measured by CBA assay. Two-way ANOVA with Tukey's multiple comparisons was used (n=3 for AAV-CAR Treg and polyclonal Treg treated groups, n=2 for the PBS treated group for A, B, C, D, E, F, G, H, I, J, K, L and M). Error bars are mean  $\pm$  SEM; \*  $p \leq 0.05$ , \*\*  $p \leq 0.01$ , \*\*\*  $p \leq 0.001$ , \*\*\*\*  $p \leq 0.0001$ .



**Table S1. Cell count and Viability for the proliferation assay.**

		<b>Sample Name</b>	<b>Viability (Percentage of Singlets)</b>	<b>Cell Count</b>
<b>Day 3</b>	<b>anti-CD3-CD28</b>	AAV-CAR T cells (Donor 1)	98	100100
		AAV-CAR T cells + AAV-CAR Tregs (Donor 1)	98.1	195878
		AAV-CAR T cells (Donor 2)	98.9	117302
		AAV-CAR T cells + AAV-CAR Tregs (Donor 2)	97.8	196120
		AAV-CAR T cells (Donor 3)	99	40911
		AAV-CAR T cells + AAV-CAR Tregs (Donor 3)	99.4	47780
	<b>AAV1-HEK</b>	AAV-CAR T cells (Donor 1)	93.4	96968
		AAV-CAR T cells + AAV-CAR Tregs (Donor 1)	97.3	195720
		AAV-CAR T cells (Donor 2)	96.4	99583
		AAV-CAR T cells + AAV-CAR Tregs (Donor 2)	96.9	196691
		AAV-CAR T cells (Donor 3)	97.8	46537
		AAV-CAR T cells + AAV-CAR Tregs (Donor 3)	99.3	46311
<b>Day 5</b>	<b>anti-CD3-CD28</b>	AAV-CAR T cells (Donor 1)	97.9	180844
		AAV-CAR T cells + AAV-CAR Tregs (Donor 1)	97.9	354395
		AAV-CAR T cells (Donor 2)	98.3	173387
		AAV-CAR T cells + AAV-CAR Tregs (Donor 2)	98.2	309298
		AAV-CAR T cells (Donor 3)	84.4	38975
		AAV-CAR T cells + AAV-CAR Tregs (Donor 3)	74.8	43057
	<b>AAV1-HEK</b>	AAV-CAR T cells (Donor 1)	97.8	177301
		AAV-CAR T cells + AAV-CAR Tregs (Donor 1)	97.5	346558
		AAV-CAR T cells (Donor 2)	97.4	168404
		AAV-CAR T cells + AAV-CAR Tregs (Donor 2)	97.8	295042
		AAV-CAR T cells (Donor 3)	73.1	42966
		AAV-CAR T cells + AAV-CAR Tregs (Donor 3)	74.6	43378

**Table S2. Antibodies used for immunofluorescence.**

Target	Fluorophore	Target Species	Clone	Vendor	Catalogue Number
CD4	Brilliant Violet 605	Anti-human	OKT4	Biolegend	317438
CD8a	Brilliant Violet 605	Anti-human	SK1	Biolegend	344741
CD19	APC	Anti-human	HIB19	Biolegend	302212
CD4	PerCP/Cyanine5.5	Anti-human	OKT4	Biolegend	317428
CD8a	PerCP/Cyanine5.5	Anti-human	HIT8a	Biolegend	300924
LAP	PE	Anti-human	TW4-2F8	BD Biosciences	562260
FoxP3	FITC	Anti-mouse	FJK-16s	Thermo/ebio	11-5773-82
GARP	Brilliant Violet 605	Anti-mouse	7B11	BD Biosciences	742801
Live Dead Violet				Thermo/ebio	L34964
CD25	PE/Cyanine7	Anti-human	BC96	Biolegend	302612
Neuropilin-1 (CD304)	PerCP-eFluor 710	Anti-human	TNKUSOHA	Thermo/ebio	46-3049-42
CTLA4 (CD152)	PE	Anti-human	BNI3	Biolegend	369604
GITR (CD357)	APC-eFluor 780	Anti-human	eBioAITR	Thermo/ebio	47-5875-42

- Keeler, A.M., Conlon, T., Walter, G., Zeng, H., Shaffer, S.A., Dungtao, F., Erger, K., Cossette, T., Tang, Q., Mueller, C., and Flotte, T.R. (2012). Long-term correction of very long-chain acyl-coA dehydrogenase deficiency in mice using AAV9 gene therapy. *Molecular therapy : the journal of the American Society of Gene Therapy* 20, 1131-1138. 10.1038/mt.2012.39.